Hindawi
Structural Control and Health Monitoring
Volume 2023, Article ID 2488951, 16 pages
https://doi.org/10.1155/2023/2488951

Research Article

Finite Element Model Updating of Bridge Structures Based on Improved Response Surface Methods

Ying Zhao[1], **Jingjing Zhang**[1], **Dongsheng Li**[2], **Daocheng Zhou**[1] and **Dabo Xin**[3]

[1]*Northeast Forestry University, Harbin, China*
[2]*Dalian University of Technology, Dalian, China*
[3]*Hainan University, Haikou, Hainan, China*

Correspondence should be addressed to Dongsheng Li; lidongsheng@dlut.edu.cn

Received 9 December 2022; Revised 28 February 2023; Accepted 15 March 2023; Published 28 March 2023

Academic Editor: Jun Li

An accurate and reasonable finite element model is essential for bridge structural health monitoring and safety assessment. To improve the accuracy and efficiency of the finite element model updating, this paper proposes a finite element model updating method for bridge structures based on an improved response surface method. By introducing the radial basis function as the augmentation term of the polynomial function, a response surface model based on the augmentation polynomial is established, and the fitting accuracy of the global response surface model is improved. The convergence speed and accuracy of the response surface model optimization solution are improved by improving the regression step and annealing strategy in the simulated annealing algorithm. The method is validated using the numerical case of a simply supported beam and the finite element model of the main bridge of the Tonghe Songhua River Highway Bridge (Tonghe Bridge), and the safety condition of the main bridge of the Tonghe Bridge is evaluated using the updated finite element model. The results show that the maximum relative error of the updated parameters of the simply supported beam decreased from 13.011% before improvement to 0.719% after improvement, and the maximum relative error of the natural frequencies decreased from 0.728% before improvement to 0.225% after improvement; the maximum relative error of the natural frequencies of the finite element model of the Tonghe Bridge main bridge decreased from 21.68% before improvement to 4.23% after improvement. In April, May, and June of 2021, the main bridge of the Tonghe Bridge operated well and had a good security reserve.

1. Introduction

With China's expanding development in transportation, the number and scale of bridges in China are among the highest in the world. By the end of 2019, the country's highway bridges had reached 878,300, an increase of 3% over the previous year, of which there were 5,716 extra-large bridges and more than 100,000 long-span bridges [1]. During operation, bridges are inevitably subjected to complex and harsh environmental effects and increasing traffic loads, resulting in a decrease in their durability and load-bearing capacity, which, if not repaired in a timely manner, will not only affect the safety of pedestrians and pedestrian traffic but also shorten the service life of the bridge, which may even result in bridge collapse accidents. For example, on June 29, 2009, the Hulan River Bridge in Tieli City, Heilongjiang Province collapsed owing to the old age of the bridge, days of heavy rain, and vehicle overload, which caused 21 people to fall into the water, resulting in four deaths and four severe injuries. On April 12, 2011, the Xinjiang Peacock River Bridge collapsed owing to the fracture of the second boom of the main span, which caused the third, fourth, and fifth short T-beams of the main span to fall into the river, resulting in the collapse of the bridge roadway. On April 24, 2021, the Luoyang Yiyang Lingshan Luo River pedestrian landscape bridge was washed out because of excessive water flow, resulting in the collapse of the fourth span and deformation of the steel structure. All these bridge accidents caused significant economic losses, severe casualties, and negative social impacts. Thus, the structural health monitoring and

safety assessment of bridges must be conducted to guarantee the reliability, safety, and durability of bridge structures throughout their service life. Through the deployment of different types of sensors on the bridge to collect data signals in real time under the operational status of the structure, a bridge structure health monitoring system is used for damage identification and safety assessment. However, the real-time monitoring of each part of the bridge is impossible because of the limited number of sensors deployed in the bridge structural health monitoring system. Finite element models for analyzing bridge structural performance must be constructed to better assess the health status of bridge structures. The finite element model is frequently built based on the design information; however, after a period of service, the bridge structure will have a reduced stiffness owing to the accumulation of damage, resulting in errors in the design information. Therefore, the initial finite element model cannot accurately reflect the actual state of the actual bridge during operation. As a result, to improve the accuracy of the finite element model calculation and analysis, the initial finite element model of the structure should be updated reasonably and accurately [2, 3].

Updating the finite element model involves modifying the relevant parameters of the initial finite element model using static and dynamic experimental measurements of the structural response under the premise of ensuring the accuracy of the modal parameters; thus, the updated finite element model can reflect the actual force state of the structure [4]. Finite element model updating methods can be divided into two types: matrix and design parameters. The matrix-based model updating method primarily modifies the stiffness matrix and mass matrix of the structure. The continuity and symmetry of the updated matrix are destroyed, and the physical meaning is unclear, which limits its engineering application. The updating method based on design parameters primarily modifies the physical parameters, geometric parameters, and boundary conditions of the structure, which have the characteristics of clear physical meaning and clear optimization search direction, making it a more widely used method currently. The design parameter-based model updating method primarily includes a sensitivity analysis and response surface methods. The model updating method based on sensitivity analysis constructs a sensitivity relationship matrix between the structural response values and design parameters and then iteratively optimizes them with the finite element model. In 2014, Billmaier et al. [5] performed model updating for continuous steel beams based on the sensitivity method to explore the relationship between the reliability of the sensitivity model updating method and the response stimulate method, and the results showed that the stimulate method of the structural response increases the instability of the updating results and makes the updating results not reliable. In 2015, Shadan et al. [6] proposed a sensitivity equation to reduce the adverse effect of frequency response data on the model updating based on the sensitivity-based model updating method and verified the effectiveness of the method by establishing a numerical model of the truss, and the results showed that the method can effectively model the updated structure in the presence of measurement errors and incomplete measurement data. In 2018, Bartilson et al. [7] combined Bayesian regularization theory in order to improve the sensitivity-based model updating method and validated the effectiveness of the method by applying it on numerical models of trusses as well as actual engineering of suspension bridges, and the results showed that the method can improve the instability of the sensitivity-based model updating method, which is less efficient in calculation, slower in convergence, and less effective in convergence. The response surface method uses regression analysis to fit the response values or test values at the sample points in the design space to obtain the response surface model simulating the actual state and to acquire the optimal model updating parameters through the optimal solution. The response surface method is widely used to update finite element models because of its high computational efficiency and clear physical meaning in engineering applications. In 1951, Box and Wilson [8] proposed the response surface method, which was primarily applied in the chemical industry to solve the problem of optimality conditions in chemical research, and they indicated that the response surface method is applicable in other fields involving optimization problems. In 1995, Myers and Anderson-Cook [9] summarized the development and application of the response surface methodology and defined it as a mathematical analysis method that can be used for development, improvement, and optimization. In recent years, the response surface method has been widely used in updating the finite element models of engineering structures. In 2017, Marwala et al. [10] performed model updating for asymmetric *H*-shaped structures by optimizing the response surface model in combination with simulated annealing and genetic algorithms, and the results showed that the simulated annealing algorithm and the genetic algorithm have similar computational accuracy. In 2020, Alpaslan et al. [11] applied the response surface method to the historical masonry spire structure model, and after the updated, the value of the frequency error of the structure was reduced from 10.59% to 5.06%, indicating that the updated finite element model of the structure agreed well with the experimental results, verifying the applicability of the response surface method on historical civil engineering structures. In 2005, Guo Qin-tao and Qing-guo [12] analyzed the influence of the experimental design options on the regression accuracy of the response surface model through four nonlinear explicit functions and an H-beam finite element arithmetic example. The results showed that the *D*-optimization experimental design method has a high regression accuracy and high reliability and is suitable for high-order and multivariate regression. In 2008, Huabing and Weixin [13, 14] applied the response surface method to update the finite element model of the Hongtang Bridge, and the results showed that the response surface method can significantly improve the efficiency of model updating and that the calculation method is simple and easy to apply in engineering practice. In 2012, Zhouhong et al. [15, 16] combined the response surface method with bridge structural health monitoring and successfully updated the model for the Lower Baishi Bridge,

thereby verifying the feasibility of the response surface method in the field of bridge health monitoring. In 2017, Dong et al. [17, 18] adopted a higher-order polynomial, exponential function, power function, and multiple adaptive regression spline function for response surface model updating and observed that the quadratic polynomial function can achieve a balance between the fitting accuracy and computational efficiency, which has a good engineering application. In 2021, Aborehab et al. [19] used a genetic algorithm, adaptive multiple optimization, and response surface method for the model updating of honeycomb sandwich structures, and the results showed that the response surface method is suitable for model updating of composite structures with high computational efficiency. In 2021, Cheng and Song [20] used a quadratic polynomial response surface model to update the model of the Yingzhou Bridge and observed that improving the fitting function of the response surface model can effectively improve the fitting accuracy of the response surface model. The literature study about response surface methods shows that the finite element model updating using response surface method is characterized by high computational efficiency and clear physical meaning of updating parameters, but problems still exist, such as limited fitting accuracy due to the unreasonable establishment of response surface model and nonunique solutions due to the reduction of accuracy and validity of response surface models. Therefore, how to find a reasonable and effective response surface model needs to be further studied.

The selection of the optimal solution algorithm for the response surface model is a key factor affecting the accuracy of finite element model updating [21, 22]. The simulated annealing algorithm is a stochastic optimization algorithm based on an iterative solution strategy. The basic concept of its optimization strategy is to simulate the annealing principle in thermodynamics, with good global optimization capability and the ability to parallelly solve problems, which can ensure sufficient iteration under the premise of high optimization efficiency; thus, it is prominent among many intelligent algorithms [23, 24]. In 1998, Levin and Lieven [25] used simulated annealing and genetic algorithms to update the finite element model of a flat-wing structure, and the results showed that the simulated annealing algorithm has a higher solution accuracy and is more suitable for updating the finite element model of this type of structure. In 2003, Changlin et al. [26] proposed a simulated annealing algorithm for solving multiobjective optimal solutions through the rational design of the search strategy and parameters in the simulated annealing algorithm and verified the effectiveness of their algorithm by solving four explicit functions. In 2016, Yu [27] combined the response surface method with the simulated annealing algorithm using the residuals of the instantaneous characteristic quantity of the structural dynamic response as the objective function to rapidly update the nonlinear finite element model of a reinforced concrete shear wall structure, and they verified the effectiveness of the combination of the simulated annealing algorithm and response surface method. In 2018, Da-hua et al. [23] updated the nozzle dynamics model and reduced the relative error of the model's natural frequency to less than 2% by adding a local search process to the simulated annealing algorithm to improve the algorithm solution accuracy, which verified the effectiveness of the updating strategy. In 2019, Yuan et al. [28] solved the nonlinear parameters of a bolted cantilever beam using a simulated annealing algorithm and verified the feasibility and effectiveness of the simulated annealing algorithm by comparing and analyzing the updated results with experimental data. In 2022, Wang et al. [29] combined a simulated annealing algorithm with an agent model to successfully update the model of a spatial truss structure, and they validated the feasibility of combining the simulated annealing algorithm with the agent model. The literature analysis shows that the response surface model optimization solution using the simulated annealing algorithm has strong noise immunity and engineering applicability. However, there are fewer improvements to the simulated annealing algorithm on this basis, and the problems of low convergence accuracy and slow convergence speed exist in the simulated annealing algorithm, so it is necessary to make reasonable and effective improvements to the simulated annealing algorithm.

In this paper, an improved response surface method is proposed to update the finite element model of a bridge structure by establishing an augmented polynomial-based response surface model and improving the regression step and annealing strategy in the simulated annealing optimization solution algorithm, which aids in improving the update accuracy and efficiency. The method was validated using numerical calculations of a simply supported beam and finite element model updating of the main bridge over the Tonghe River.

2. Basic Method of Finite Element Model Updating

2.1. Response Surface Model with Augmented Polynomials. Finite element model updating based on the response surface method frequently adopts a quadratic polynomial to establish the response surface model reflecting the relationship between the structural design input and response output, and its expression is shown in equation (1). The quadratic polynomial response surface model can achieve a balance between fitting accuracy and computational efficiency; therefore, it is widely used in engineering, but the fitting accuracy is often low when used to construct a global response surface model for structures, resulting in unstable model predictions. Radial basis functions are also more effective when used to construct response surface models, particularly in building global explicit models of nonlinear functions; however, they are limited to the design space range and have poor engineering applicability. Thus, the introduction of a radial basis function as an augmentation term of the polynomial function can improve the fitting accuracy of constructing the global response surface model and satisfy a wider range of engineering applications.

$$y(x) = \beta_0 + \sum_{i=1}^{k} \beta_i x_i + \sum_{i=1}^{k} \sum_{j=1}^{k} \beta_{ij} x_i x_j, \tag{1}$$

where $x \in [x_i^l, x_i^u]$, $(i \in (1,k))$, x_i^l is the upper boundary of the range of values of the design parameter x_i, x_i^u is the lower boundary of the range of values of the design parameter x_i, and $\beta_0, \beta_i, \beta_{ii}, \beta_{ij}$ are the coefficients to be determined.

By testing different types of functions to be fitted, we observe that the Gaussian radial basis function can maintain a stable and small error value among many radial basis functions, indicating that the Gaussian radial basis function has good fitting adaptability, high accuracy, and wide applicability [30]. The Gaussian radial basis function is used as an augmentation term of the polynomial function to obtain a response surface model with high accuracy, and the expression of the Gaussian radial basis function is shown in the following equation:

$$s(x) = \sum_{j=1}^{m} \lambda_j \exp\left(-c\left\|x - x^{(j)}\right\|^2\right), \tag{2}$$

where m is the number of interpolated sample points, $x^{(j)}$ is the set of sample points generated by the experimental design, $\{x^{(j)} \in E^n | j = 1, 2, \cdots, m\}$, $\lambda_j (j = 1, \cdots, m)$ is the coefficient to be determined, c is a constant set according to the empirical formula [31], and $0 < c \leq 1$ and $\|x - x^{(j)}\|$ are the distance from any point on the interpolation function to the jth interpolated sample point, which is the Euclidean parameterization.

In summary, the response surface model based on the augmented polynomial is shown in the following equation:

$$F(x) = y(x) + s(x) = \beta_0 + \sum_{i=1}^{k} \beta_i x_i + \sum_{i=1}^{k} \sum_{j=1}^{k} \beta_{ij} x_i x_j + \sum_{j=1}^{m} \lambda_j \exp\left(-c\left\|x - x^{(j)}\right\|^2\right). \tag{3}$$

2.2. Improved Simulated Annealing Algorithm. With a simulated annealing algorithm for the optimal solution of response surface models, the search step size is fixed, which limits the computational efficiency, and the single treatment strategy for nonoptimal solutions in the annealing strategy prevents it from jumping out of the local optimal dilemma. To improve the convergence speed and accuracy, we improve the regression step and annealing strategy of the simulated annealing algorithm

The adaptive regression coefficients are constructed in the regression step, and the fixed values are replaced by self-adaptive values, which gradually decrease with an increase in the number of iterations. This not only expands the search range and improves the computational efficiency but also ensures a delicate solution and an optimal solution in the global range. The self-adaptive value expression is shown in the following equation:

$$\alpha(t) = \alpha_{\max} \exp\left[\frac{t_{sp}}{T_{\max}} \ln\left(\frac{\alpha_{\min}}{\alpha_{\max}}\right)\right], \tag{4}$$

where $T_{\max}$ is the total number of iterations, t_{sp} is the current number of iterations, $\alpha_{\min}$ is the minimum step size calculated in the regimen space, $\alpha_{\max}$ is the maximum step size, and t is the number of iterations.

When iterative calculations are performed in the annealing strategy, the worst performing solution is accepted according to a certain probability, and discriminating whether there is a superior solution in the vicinity of that worst solution to ensure that the optimal solution is sought in the global range. The solution acceptance probability expression is shown in the following equation:

$$p = \begin{cases} 1, & E_j < E_i, \\ \exp\left(\dfrac{E_i - E_j}{T}\right), & E_j > E, \end{cases} \tag{5}$$

where p is the solution acceptance probability, E_i is the function output value corresponding to X_i before ingestion, E_j is the function output value corresponding to new solution X_j after ingestion, and T is the current state temperature.

The flowchart of the improved simulated annealing algorithm is shown in Figure 1.

2.3. Model Updating Process. The main steps for updating the finite element model based on the improved response surface method are as follows:

(1) Selection of parameters for updating the model. The parameters to be updated are listed according to the actual engineering scenario, and the parameters with higher sensitivity are selected as the parameters of the finite element model updating. The formula for calculating the sensitivity of the parameters to be updated to the structural response values is shown in the following equation:

$$\frac{\partial E_i}{\partial x_i} = \frac{\Delta E_i / E_i}{\Delta x_i / x_i}, \tag{6}$$

where x_i is the parameter value to be updated, E_i is the corresponding response value, ΔE_i is the small regurgitation value of the response, and Δx_i is the small regurgitation value of the parameter to be updated.

(2) Selection of sample points. After determining the design space of the design parameters, the design of the experimental method is used to generate sample points and substitute them into the structural finite element model for iterative calculations to obtain the corresponding response values.

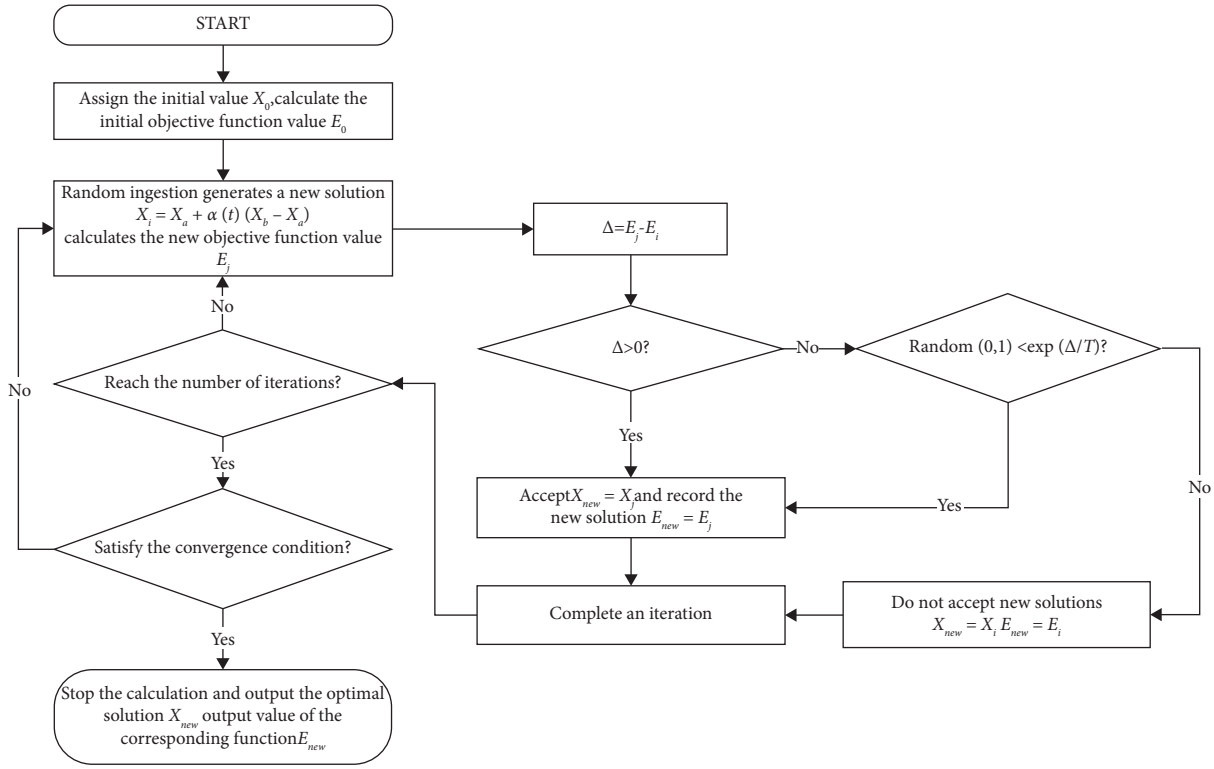

Figure 1: Flowchart of the improved simulated annealing algorithm.

(3) Establishment of response surface model. First, quadratic polynomials are used for the initial fitting of the structural finite element model. Subsequently, the Gaussian radial basis function is used to eliminate the error between it and the finite element model. Finally, a response surface model based on the augmented polynomial is obtained.

(4) Testing the response surface model. The accuracy of the response surface model is tested using the root mean squared error sum (RMSE), and the closer the value of the RMSE is to 0, the more accurate the response surface model. The RMSE is calculated as follows:

$$\mathrm{RMSE} = \sqrt{\sum_{i=1}^{k} \frac{\left(\overline{F^{(i)}} - F^{(i)}\right)^2}{K}}, \tag{7}$$

where K is the number of noninterpolated sample points, $F^{(i)}$ is the sample value of the ith point among the sample points, and $\overline{F^{(i)}}$ is the response value obtained from the response surface model corresponding to the ith point among the sample points.

(5) Solving the optimization. The optimized solution is solved using an improved simulated annealing algorithm, and the error of its optimal solution is determined when it reaches the convergence state, and then, the optimized result is output if it satisfies the requirements.

The flowchart of the finite element model updating based on the improved response surface method is shown in Figure 2.

3. Numerical Case Study

3.1. Establishment of Finite Element Model of a Simply Supported Beam. The calculated span of the simply supported beam was 15 m, and the dimensions of the rectangular section of the box beam were 250 mm (height) × 200 mm (width) × 50 mm (thickness). The finite element model of the simply supported beam was established using the finite element calculation software ABAQUS and divided into 15 elements that element type of finite element model of simply supported beam is beam element. The modulus of elasticity of the material was 3.55×10^4 MPa, the density was 2.550 KN/m^3, and Poisson's ratio was 0.2. The damage to the simply supported beams was simulated by reducing the modulus of elasticity of the material, and the moduli of elasticity of units 5, 9, and 15 were reduced by 27%, 10%, and 16%, respectively. A damage diagram of the simply supported beam is shown in Figure 3. The dynamic calculation of the finite element model was performed using ABAQUS, and the vertical forward fourth-order vibration frequencies of the simply supported beam were obtained as 0.8965, 2.4365, 4.8052, and 7.9238 Hz, respectively.

3.2. Finite Element Model Updating of the Simply Supported Beam. The modulus of elasticity of the 1/4 span (cell 4), 1/2 span (cell 8), 3/4 span (cell 12), and damaged cells (cells 5, 9,

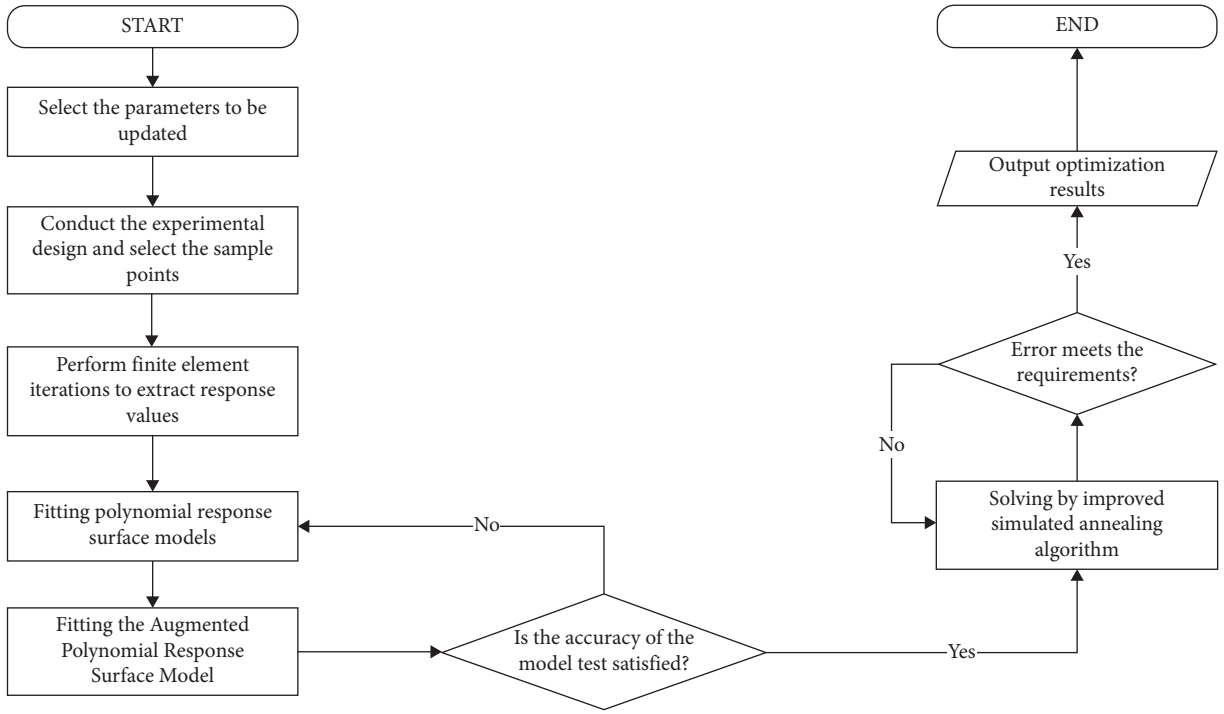

Figure 2: Flowchart of the finite element model updating process based on the improved response surface method.

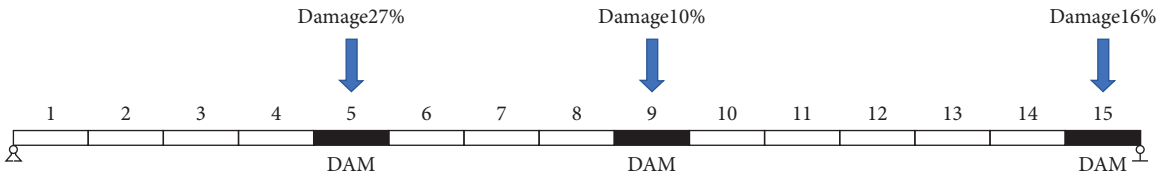

Figure 3: Diagram of damage of a simply supported beam.

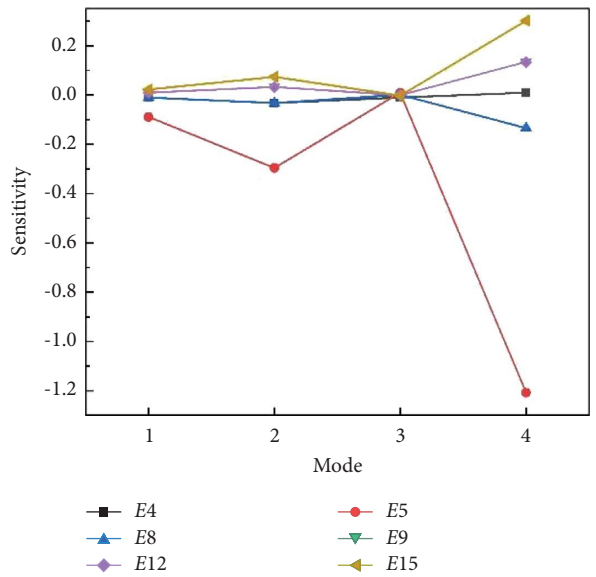

Figure 4: Sensitivities of the parameters to be updated to the natural frequencies.

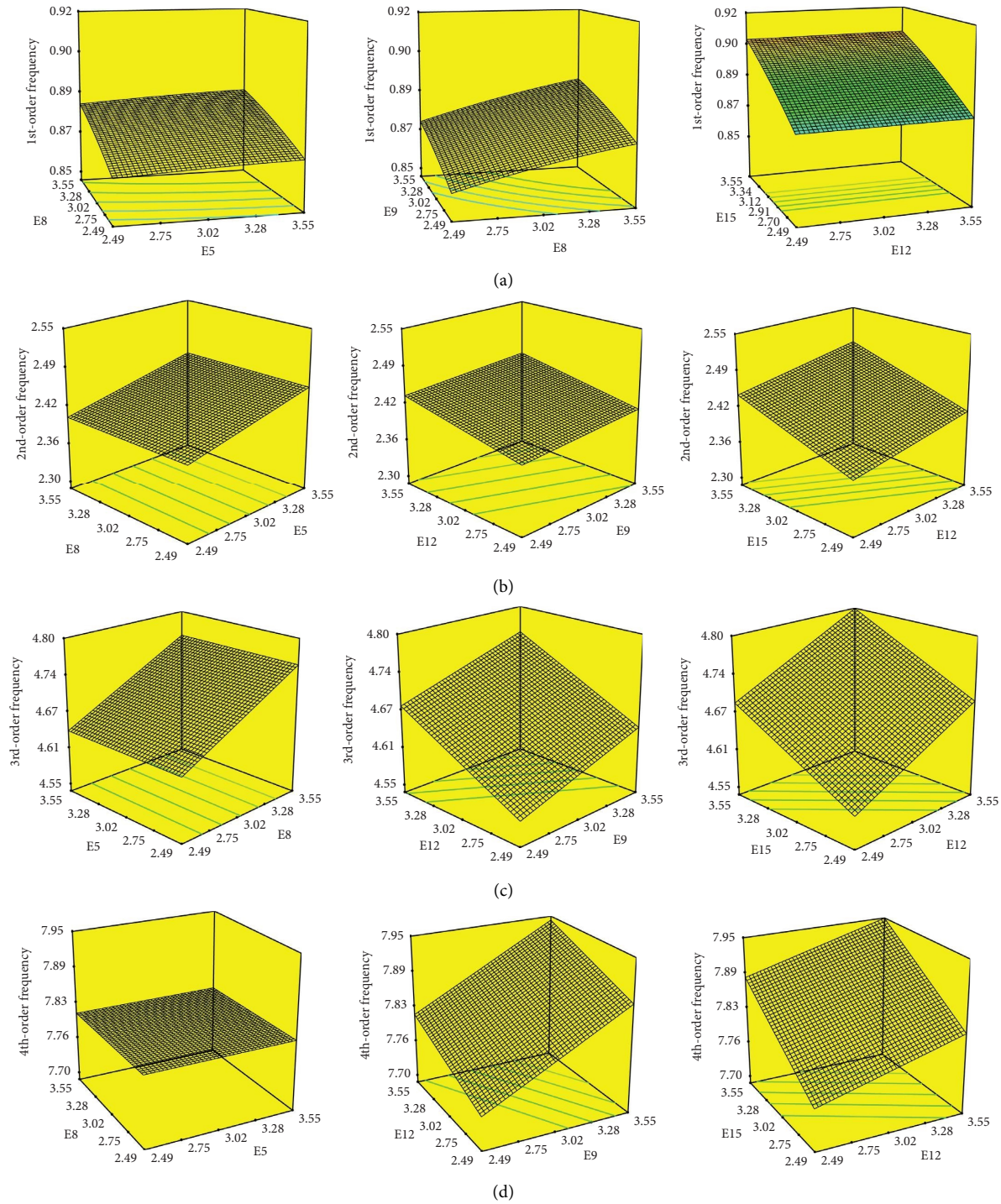

Figure 5: Augmented polynomial-based response surface model for the natural frequencies of the simply supported beam: (a) vertical first-order frequency response surface model, (b) vertical second-order frequency response surface model, (c) vertical third-order frequency response surface model, and (d) vertical fourth-order frequency response surface model.

and 15) of the simply supported beam was selected as the parameters to be updated, denoted as $E4$, $E5$, $E8$, $E9$, $E12$, and $E15$, respectively. The sensitivities of the parameters to be updated to the natural frequencies are shown in Figure 4. The sensitivity of $E4$ was approximately 0, which means that the effect of this parameter on the natural frequency response of the simply supported beam was very small and could be ignored; thus, $E5$, $E8$, $E9$, $E12$, and $E15$ were selected as the updating parameters.

Considering the actual damage of the simply supported beam, the design space of the updating parameters was set to (2.485, 3.55), the D-optimization experimental design method was used to generate five-factor sample points, and a dynamic analysis of the finite element model was

performed to obtain the structural natural frequencies, which constituted the output response of the sample points, and the response surface model of the first four orders of natural frequencies of the simply supported beam based on the augmented polynomial was established (Figure 5).

The RMSE values of the first fourth-order natural frequency response surface models of the simply supported beam were 0.0002, 0.0193, 0.0417, and 0.0363, respectively, which showed that the RMSE values tended to be close to 0, indicating that the established response surface models were precise. The relative error sum of the squared calculated and measured frequencies was selected as the objective function, and an improved simulated annealing algorithm was used to determine the optimal solution. The results of the optimal solution with these parameters are listed in Table 1.

3.3. Validation of the Model Updating Method. Figure 6 compares the RMSE values of the response surface models based on the quadratic and extended polynomials for the first four orders of the natural frequencies of the simply supported beam. Furthermore, Figure 6 shows that the RMSE values of the response surface models based on the augmented polynomial were smaller than those of the quadratic polynomial response surface model, indicating that the fitting accuracy of the augmented polynomial response surface model was higher than that of the quadratic polynomial response surface model.

The convergences of the iterations using the traditional and improved simulated annealing algorithms to optimize the response surface model of the simply supported beam are shown in Figure 7. When the traditional simulated annealing algorithm was used to optimize the solution of each parameter, it easily fell into a stagnant state during the iterative process, and the calculation results could not converge to the true value, with a slow convergence speed and low convergence accuracy. When the improved simulated annealing algorithm was used to optimize the solution of each parameter, it converged in approximately 100 iterations, and the calculation results all converged to the unique true value, indicating that the improved simulated annealing algorithm has a high convergence speed and high convergence accuracy.

The parameter-updated results based on the different model updating methods are shown in Table 2 and Figure 8. The maximum relative error of the updated parameter values of the finite element model based on the traditional response surface method was 13.011%, and the maximum relative error of the updated parameter values of the finite element model based on the improved response surface method was 0.719%, which was 12.292% lower than the former, indicating that the accuracy of the updated finite element model based on the improved response surface method was higher.

Table 3 shows a comparison of the natural frequencies of the simply supported beam based on different model updating methods. After the finite element model was updated based on the traditional response surface method, the maximum relative error of the natural frequencies of the simply supported beam was 0.728%. The maximum relative error of the natural frequencies of the simply supported beam after the finite element model update based on the improved response surface method was 0.225%, which was 0.503% lower than that of the former. The updated finite element model based on the improved response surface method was closer to the actual force state of the structure.

Table 1: Results of the updated parameter solution.

Parameters	$E5$	$E8$	$E9$	$E12$	$E15$
Initial value	3.550	3.550	3.550	3.550	3.550
Optimal solution ($\times 10^4$ MPa)	2.580	3.550	3.236	3.550	2.967

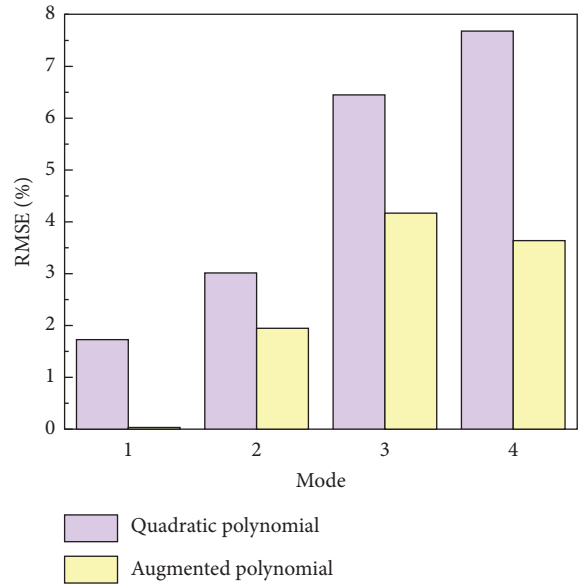

Figure 6: RMSE values of frequencies response surface model of simply supported beam.

3.4. Noise Effects on Model Updating Results. In order to verify the robustness of the updated method, Section 3.4 has been added to the manuscript, and the content is as follows.

In order to test the influence of noise on the proposed model correction method, a certain level of Gauss white noise was added to the dynamic response of the structure to simulate the noise pollution on the data and analyze its influence on the correction results. The dynamic response of the structure with noise can be expressed as follows:

$$x_{\text{noise}} = x + E_P \sigma(x) N_{\text{noise}}, \tag{8}$$

where x_{noise} is the processed noisy response, x is the original response, E_P is the noise level, $\sigma(x)$ is the standard deviation of the original response, and N_{noise} is a random array with zero mean and variance of 1 consistent with the length of the original data.

The results of model updating under different noise levels are shown in Figure 9. From Figure 9, for the updated results of the updated parameters, the maximum relative errors under different noise levels are 2.651% and 6.368%,

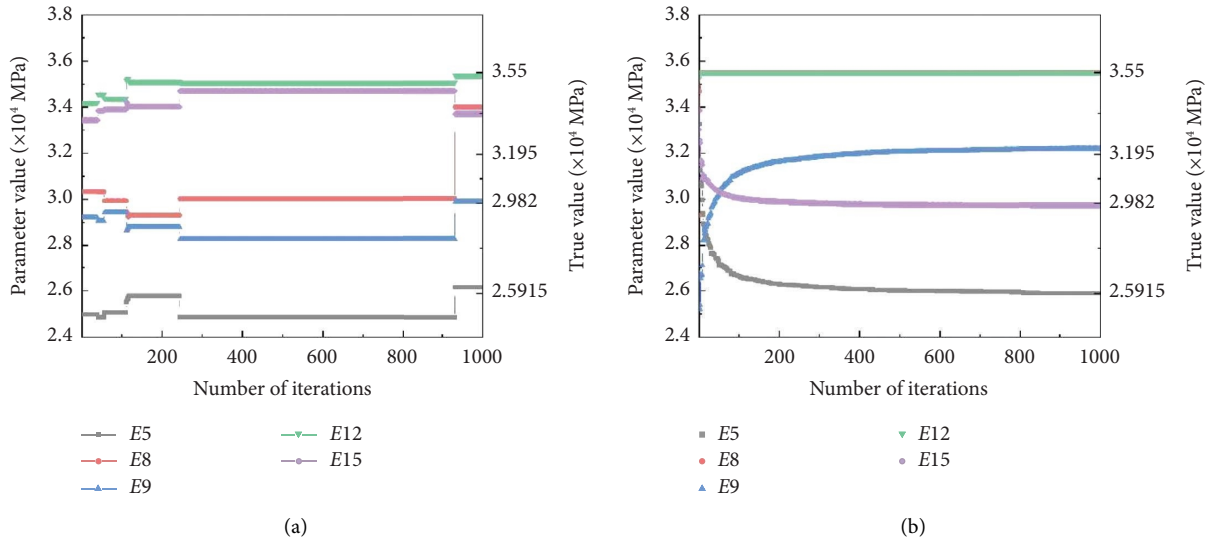

Figure 7: Convergence of the iterations based on different algorithms: (a) traditional simulated annealing algorithm and (b) improved simulated annealing algorithm.

Table 2: Comparison of parameter-updated results based on different model updating methods.

Parameters	True value ($\times 10^4$ MPa)	Traditional response surface method		Improved response surface method	
		Updated ($\times 10^4$ MPa)	Error (%)	Updated ($\times 10^4$ MPa)	Error (%)
$E5$	2.592	2.617	0.984	2.591	0.019
$E8$	3.55	3.399	4.254	3.550	0
$E9$	3.195	2.987	6.510	3.218	0.719
$E12$	3.55	3.537	0.366	3.550	0
$E15$	2.982	3.370	13.011	2.973	0.302
Converged iterations (steps)		932		97	

respectively; for the updated results of the structural natural frequency, the maximum errors under different noise levels are 1.276% and 5.697%, respectively. Comparing the updated results of 5% noise level and 10% noise level, it can be learned that the relative errors of the updated results increase with the increase of noise level, but the relative errors are all lower than 10%, which indicates that the proposed improved response surface method can effectively suppress the influence of noise on the correction results and ensure the stability of the calculation results, indicating that the method has good robustness to error pollution.

4. Finite Element Model Updating of the Main Bridge over the Tonghe River

4.1. Description of the Bridge and Monitoring System. Tonghe Bridge was completed and opened to traffic in 2009. The total length of the bridge is 2578.28 m, and the main bridge structure is a prestressed concrete continuous box girder bridge, divided into two links; the span arrangement of each link is 63 m + 4 × 110 m + 63 m, with a total length of 1132 m, as shown in Figure 10. The main bridge box girder adopts a single-box and double-chamber section, the height of the piers top of the main span is 6 m, and the height of the mid-span is 2.5 m, during which the girder height changes according of 1.65 times parabolic in the longitudinal direction. The key parts of the main bridge are monitored in real time according to the structural characteristics of the Tonghe Bridge and the actual operation conditions. The specific monitoring parts and contents are listed in Table 4.

4.2. Establishment of the Initial Finite Element Model. The initial finite element model of the main bridge over the Tonghe River was established using the finite element analysis software MIDAS CIVIL, and the ratio of the finite element model to the real bridge dimensions was 1 : 1. The entire bridge was simulated using a beam with 307 nodes and 243 units. The bottom of the bridge pier was set as a fixed restraint, the main beam was connected to the top of the middle pier with a fixed bearing, and the others were set as movable bearings along the longitudinal direction of the bridge for the simulation. The parameters of the concrete and reinforcement materials are shown in Tables 5 and 6, respectively. A finite element model of the main bridge over the Tonghe River is shown in Figure 11.

4.3. Finite Element Model Updating. The main beam concrete elastic modulus E, density ρ, and Poisson's ratio μ were selected as the updated parameters for the analysis, and the design space is listed in Table 7. The D-optimization experimental design method was used to generate three-factor

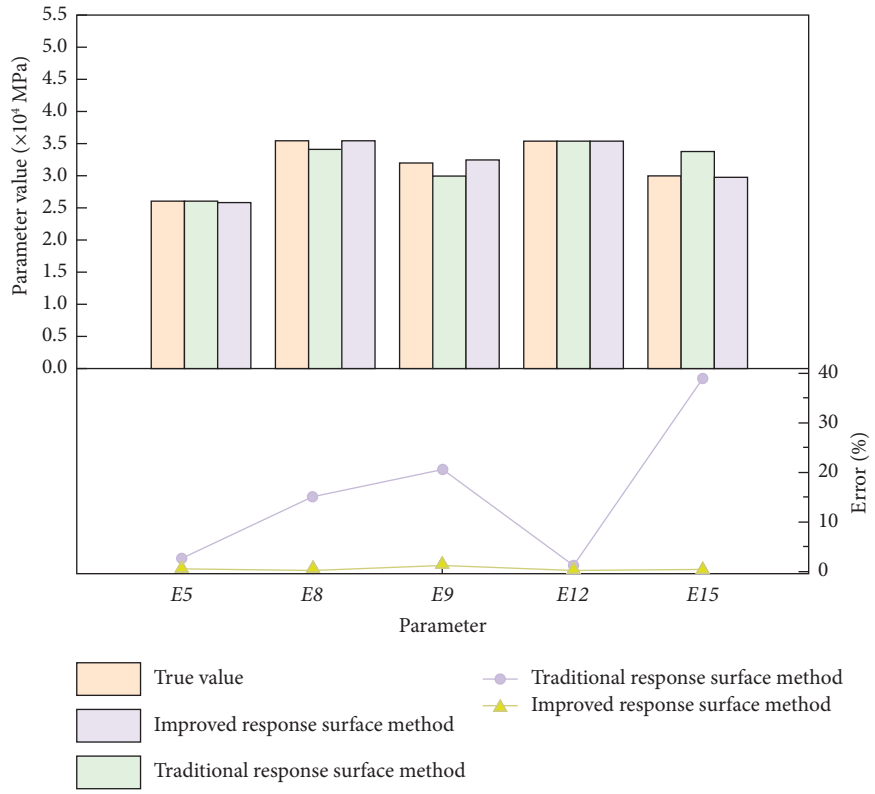

Figure 8: Results of parameter updated based on different model updating methods.

Table 3: Comparison of natural frequencies of the simply supported beams based on different model updating methods.

Frequency	True value (Hz)	Initial (Hz)	Error (%)	Traditional response surface method		Improved response surface method	
				Updated (Hz)	Error (%)	Updated (Hz)	Error (%)
1st	0.896	0.920	2.625	0.903	0.728	0.897	0.059
2nd	2.436	2.522	3.509	2.448	0.472	2.435	0.062
3rd	4.805	4.913	2.243	4.793	0.254	4.816	0.225
4th	7.924	8.056	1.668	7.922	0.023	7.926	0.028

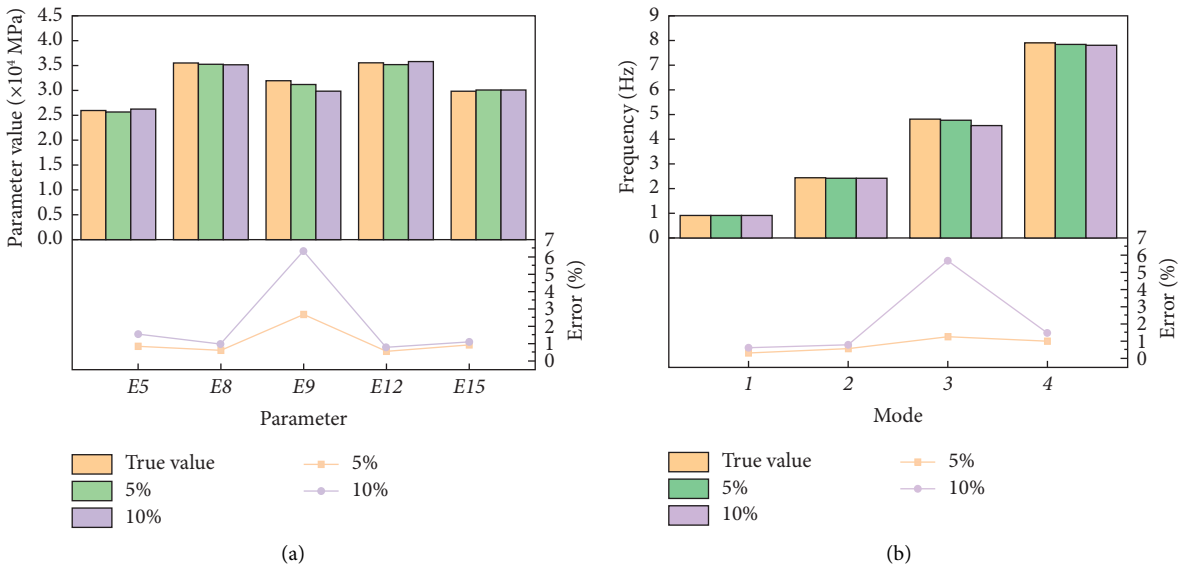

Figure 9: Results of model updating based on measurement noise with different error levels (5% and 10%): (a) parameters value result; (b) frequency result.

Figure 10: Tonghe Bridge picture.

Table 4: List of monitoring contents.

Monitoring projects	Layout location	Number of measuring points	Type of sensor
Structural vibration	Middle of main span	4	Accelerometer
Strain	Mid-span section, end-beam section	112	Vibrational chord strain gauge (with temperature)
Vertical deflection	1/4 span, 1/2 span, 3/4 span	36	Flexometer

Table 5: Parameters of concrete materials.

Concrete level	Elastic modulus E_c ($\times 10^4$ MPa)	Shear modulus G_c ($\times 10^4$ MPa)	Design value of axial compressive strength f_{cd} (MPa)	Design value of axial tensile strength f_{td} (MPa)	Standard value of axial compressive strength f_{ck} (MPa)	Standard value of axial tensile strength f_{tk} (MPa)
C60	3.6	1.44	26.5	1.96	38.5	2.85
C30	3.0	1.20	13.8	1.39	20.1	2.01

Table 6: Parameters of reinforcing steel material.

Reinforcement level	ϕ^s15.2 steel stranded wire	HRB335	R235	Q235 steel plate
Standard strength f_{sk} (MPa)	1860	335	235	235

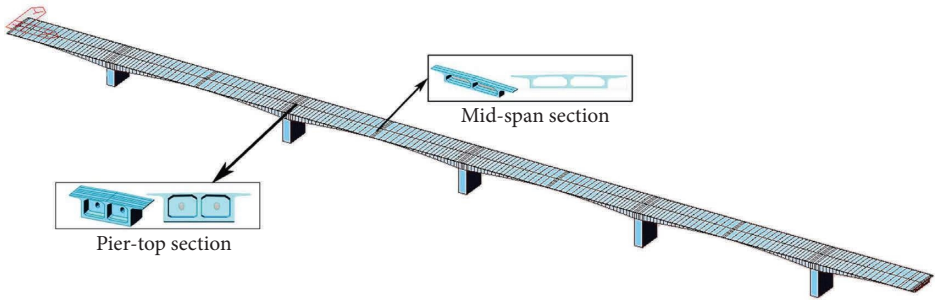

Figure 11: Finite element model of the main bridge over the Tonghe River.

sample points. Subsequently, the initial finite element model was dynamically analyzed to extract the natural frequencies of the main bridge over the Tonghe River, and the output responses corresponding to the input sample points were obtained.

The natural frequency response surface model of the main bridge over the Tonghe River, based on the augmented polynomial, is shown in Figure 12. The RMSE values of the first three orders of the natural frequency response surface model of the Tonghe Bridge were 3.47×10^{-9}, 1.09×10^{-9}, and 1.74×10^{-8}, respectively. The RMSE values of the response surface model tended to be close to zero, which indicated that the accuracy of the regression response surface model was good.

Table 7: Design space for finite element model update parameters.

Update parameters	Minimum	Maximum
Elastic modulus E ($\times 10^4$ MPa)	2.67	3.55
Density ρ (KN/m^3)	2.550	3.315
Poisson's ratio μ	0.2	0.3

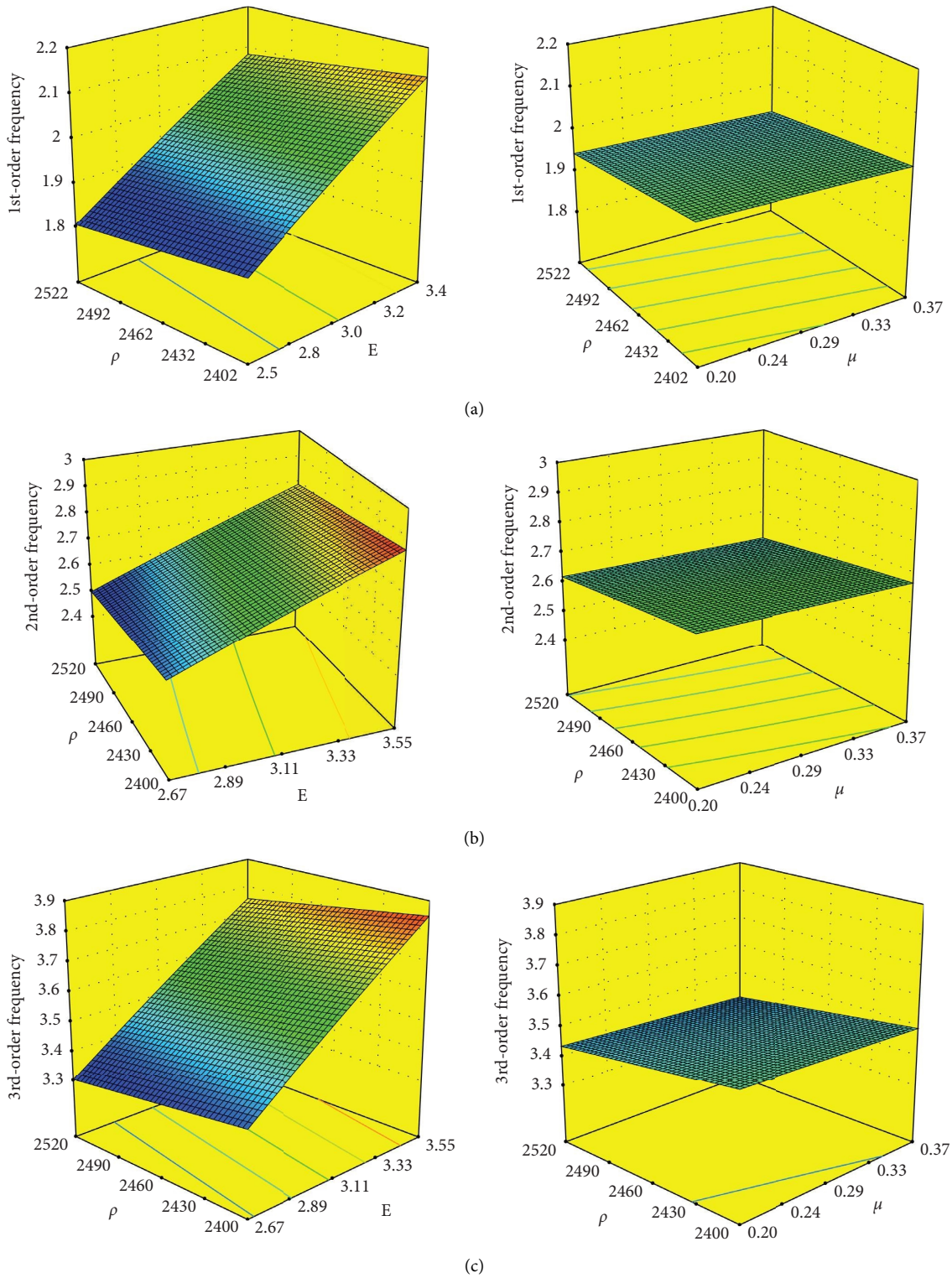

Figure 12: Natural frequencies response surface model of the main bridge over the Tonghe River based on augmented polynomials: (a) vertical first-order frequency response surface model, (b) vertical second-order frequency response surface model, and (c) Vertical third-order frequency response surface model.

Table 8: Solution result of the updated parameters.

Update parameters	Elastic modulus E ($\times 10^4$ MPa)	Density ρ (KN/m^3)	Poisson's ratio μ
Optimal solution	2.97	2.629	0.2

Table 9: Comparison of natural frequencies before/after was model updated.

Natural frequency	Measured frequency (Hz)	Before updating		Traditional response surface method		Improved response surface method	
		Frequencies (Hz)	Error (%)	Updated (Hz)	Error (%)	Updated (Hz)	Error (%)
First	1.741	2.119	21.68	1.888	8.44	1.758	0.94
Second	2.559	2.787	8.88	2.542	0.66	2.559	0.02
Third	3.371	3.763	11.64	3.635	7.83	3.229	4.23

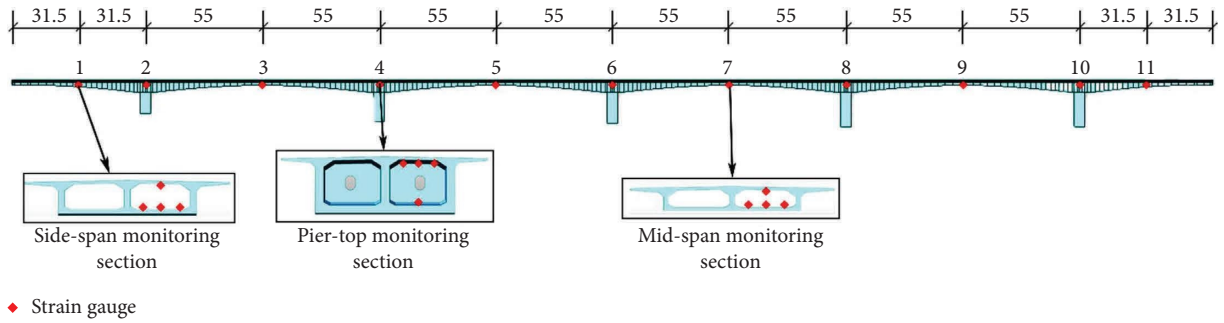

Figure 13: Layout diagram of strain measurement points (unit: m).

4.4. Analysis of Model-Updating Results. The relative error sum of the squared calculated and measured frequencies was selected as the objective function, and the improved simulated annealing algorithm was used to optimize the solutions, as shown in Tables 8 and 9, and compare the natural frequencies of the finite element model of the main bridge before and after updating. Tables 8 and 9 summarize that the updated frequencies were in good agreement with the measured frequencies, and the maximum error was 21.68% before the update and 4.23% after the update, implying that the updated FEM model was effective, and the updated bridge FEM model was more consistent with the actual condition of the bridge. As can be seen from Table 9, the maximum relative error of the parameter values of the finite element model updating based on the traditional response surface method is 8.44%, and the maximum relative error of the parameter values of the finite element model correction based on the improved response surface method is 4.23%, which is 4.21% lower than the maximum relative error of the traditional response surface model correction method, indicating that the accuracy of the finite element model correction based on the improved response surface method is higher.

4.5. Bridge Safety Assessment Based on Improved Response Surface Method. According to the design data of the Tonghe Bridge, the response values of each monitoring point of the bridge structure under the normal-use and load-carrying capacity limit states were calculated as the primary and secondary thresholds for structural safety assessment by applying the highway class-I vehicle load to the updated finite element model. The strain measurement points were placed in the mid-span and pier-top sections of each span of the main bridge over the Tonghe River, as shown in Figure 13. The actual maximum values of the strain monitoring data for the top and bottom plates of the main bridge of the Tonghe Bridge in April, May, and June 2021 were selected for comparison with the calculated thresholds, as shown in Figure 14. In Figure 14, the first-level maximum value was obtained by maximum tensile strain of bridge structure under normal service limit condition, first-level minimum value was obtained by maximum compressive strain of bridge structure under normal service limit condition, second-level maximum value was obtained by maximum tensile strain of bridge structures in the load carrying capacity limit condition, and second-level minimum value was obtained by maximum tensile strain of bridge structures in the load carrying capacity limit condition. As shown in Figure 14, the measured maximum strain values at each monitoring location of the main bridge did not exceed the calculated thresholds, indicating that the main bridge of the Tonghe River was in good operating condition.

The deflection measurement points were placed at the 1/4, 1/2, and 3/4 section positions of each span of the main bridge over the Tonghe River, as shown in Figure 15. The allowable value of deflection for the main span of the bridge

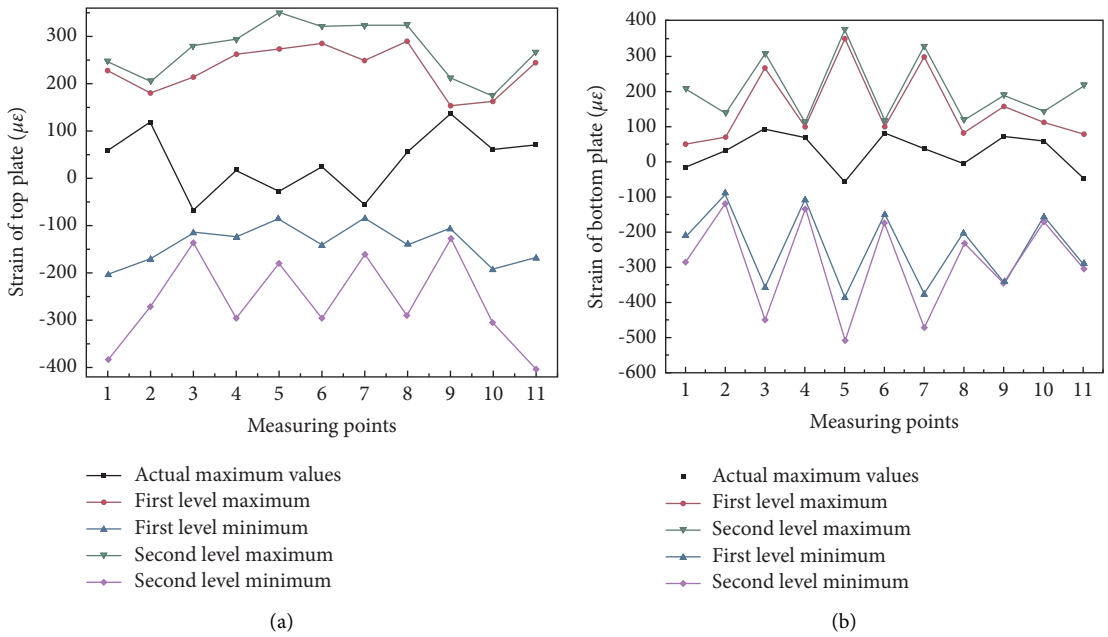

Figure 14: Comparison of the measured maximum value of strain with the calculated threshold: (a) top plate and (b) bottom plate.

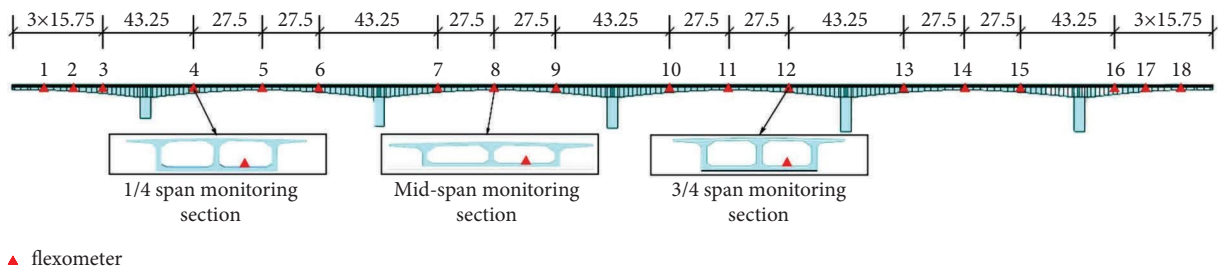

Figure 15: Layout diagram of deflection measuring points (unit: m).

was calculated as 183 mm, and the allowable value of deflection for the side spans was 100 mm, according to the specifications [32]. The maximum values of the deflection monitoring data at each measuring point of the main bridge in April, May, and June 2021 were selected for comparison with the calculated thresholds, as shown in Figure 16. In Figure 16, the first-level maximum value was obtained by vertical upward deflection of bridge structure under normal service limit condition, first-level minimum value was obtained by vertical downward deflection of bridge structure under normal service limit condition, second-level maximum value was obtained by vertical upward deflection of the bridge structure in the carrying capacity limit condition, and second-level minimum value was obtained by vertical downward deflection of the bridge structure in the load carrying capacity limit condition. As shown in Figure 16, the measured maximum values of deflection at each monitoring location of the Tonghe Bridge were much smaller than the allowable values of the code and calculated thresholds, indicating that the bridge had sufficient vertical stiffness and an adequate safety reserve in the operational condition.

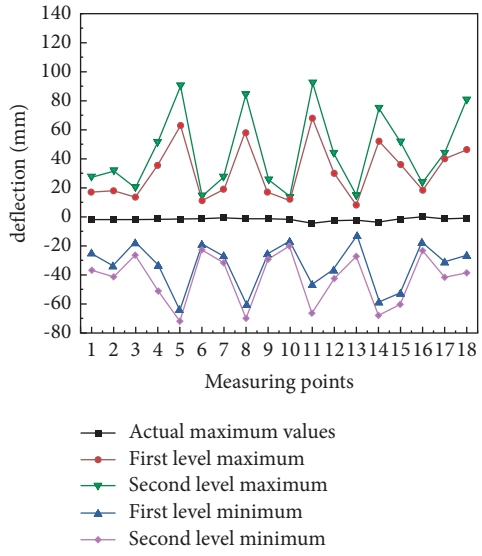

Figure 16: Comparison of the measured maximum value of deflection with the calculated threshold.

5. Conclusion

In this paper, a method for updating the finite element model of bridge structures based on the improved response surface method is proposed, and the effectiveness of the method is verified using a numerical case of a simply supported beam and the finite element model of the main bridge of the Tonghe Bridge. The safety condition of the main bridge of the Tonghe Bridge was evaluated by using the updated finite element model. The main conclusions are as follows.

(1) By introducing the radial basis function as the augmentation term of the polynomial function, a response surface model based on the augmentation polynomial is established to improve the fitting accuracy of the response surface model. The regression step in the simulated annealing algorithm is improved, and the convergence speed of the optimization solution is improved by constructing adaptive regression coefficients such that the regression value decreases with an increase in the number of iterations. The acceptance probability of the worst solution in the annealing strategy is increased to avoid the computation falling into the local optimal solution and improve the convergence accuracy of the optimization solution.

(2) The finite element model of the simply supported beam was updated using traditional and improved response surface methods. The results show that the updated finite element model based on the improved response surface method improves the fitting accuracy of the response surface model, convergence speed, and accuracy of the optimized solution. The maximum relative error of the updated parameters of the simply supported beam was reduced from 13.011% before the improvement to 0.719% after the improvement, and the maximum relative error of the natural frequencies was reduced from 0.728% before the improvement to 0.225% after the improvement. The feasibility of the improved response surface method in structural finite element model updating was verified.

(3) Based on the improved response surface method, the finite element model of the main bridge of the Tonghe Bridge was updated, and a safety assessment was performed. The results showed that the maximum error between the calculated and measured frequencies of the finite element model of the main bridge of the Tonghe Bridge was reduced from 21.68% before updating to 4.23% after updating, indicating that the updated finite element model was closer to the actual structural stress state. During April, May, and June 2021, the maximum values of the strain and deflection monitoring data of the main bridge of the Tonghe Bridge were smaller than the model calculation thresholds, indicating that the response of the bridge structure was in a safe state under the operation condition and the bridge had a certain safety reserve.

Data Availability

All data used to support the findings of this study are included within the article.

Conflicts of Interest

The authors declare that they have no conflicts of interest.

Acknowledgments

This research was supported by the Scientific and Technological Innovation Talent Program of Harbin (2017RAQXJ014).

References

[1] Ministry of Transport of the People's Republic of China, "2019 Transport industry development statistical bulletin," 2020, http://www.gov.cn/xinwen/2020-05/12/content_5510817.htm.

[2] I. Rosati, G. Fabbrocino, and C. Rainieri, "A discussion about the Douglas-Reid model updating method and its prospective application to continuous vibration-based SHM of a historical building," *Engineering Structures*, vol. 273, Article ID 115058, 2022.

[3] W. Zou-cai, D. Ya-jie, G. Bi, Y. Zi-qing, and X. Yu, "Review on nonlinear model updating for bridge structures," *Journal of Traffic and Transportation Engineering*, vol. 22, no. 2, pp. 59–75, 2022.

[4] Z. Zhou-hong and X. Zhang-hua, "Finite element model updating method of bridge combined modal flexibility and static displacement," *China Journal of Highway and Transport*, vol. 21, no. 06, pp. 43–49, 2008.

[5] M. Billmaier, C. Bucher, and C. Adam, "Selective sensitive finite element model updating: an improved approach," *Structural Control and Health Monitoring*, vol. 21, no. 8, pp. 1170–1192, 2014.

[6] F. Shadan, F. Khoshnoudian, and A. Esfandiari, "A frequency response-based structural damage identification using model updating method," *Structural Control and Health Monitoring*, vol. 23, no. 2, pp. 286–302, 2016.

[7] D. T. Bartilson, J. Jang, and A. W. Smyth, "Sensitivity-based singular value decomposition parametrization and optimal regularization in finite element model updating," *Structural Control and Health Monitoring*, vol. 27, no. 6, 2020.

[8] G. E. Box and K. B. Wilson, "On the experimental attainment of optimum conditions," *Breakthroughs in Statistics*, pp. 270–310, Springer, Berlin, Germany, 1992.

[9] M. Myers and Anderson-Cook, *Response surface methodology*, vol. 2, no. 2, pp. 128–149, 2010.

[10] Model selection in finite element model updating, "Probabilistic finite element model updating using bayesian statistics," *Mechanical Systems and Signal Processing*, vol. 25, no. 2011, pp. 24–41, 2016.

[11] E. Alpaslan, K. Hacıefendioğlu, G. Demir, and F. Birinci, "Response surface-based finite-element model updating of a historic masonry minaret for operational modal analysis," *The Structural Design of Tall and Special Buildings*, vol. 29, no. 9, 2020.

[12] Z. L. M. Guo Qin-tao and F. E. I. Qing-guo, "Response surface method and its experimental design for deterministic computer simulation," *Acta Aeronautica et Astronautica Sinica*, vol. 27, no. 1, pp. 55–61, 2006.

[13] C. Huabing and R. weixin, "Structural finite element model updating based on response surface," in *Proceedings of the Fifteenth National Conference on Structural Engineering*, pp. 242–245, Springer Nature, Switzerland AG, January 2006.

[14] R. Weixin and C. Huabin, "Response-surface based on finite element model updating of bridge structures," *China Civil Engineering Journal*, vol. 12, pp. 73–78, 2008.

[15] Z. Zhouhong, G. Minglin, and X. Zhanghua, "Finite element model validation of the continuous rigid frame bridge based on structural health monitoring Part II: FE model updating based on the response surface method," *China Civil Engineering Journal*, vol. 44, no. 3, pp. 85–92, 2011.

[16] Z. Zhouhong, G. Minglin, and X. Zhanghua, "Finite element model validation of the continuous rigid frame bridge based on structural health monitoring Part I: FE model updating based on the response surface method," *China Civil Engineering Journal*, vol. 44, no. 02, pp. 90–98, 2011.

[17] C. Dong, *Finite Element Model Updating of Bridge Structure Based on Response Surface Technology*, Chang'an University, Xi'an, China, 2017.

[18] L. Yongpeng, "Static and dynamic the finite element model updating of bridge structure based on the response surface method," *Architectural and Civil Engineering in the Graduate School of Lanzhou University of Technology*, vol. 639-640, 2013.

[19] A. Aborehab, M. Kamel, A. F. Nemnem, and M. Kassem, "Finite element model updating of a satellite honeycomb sandwich plate in structural dynamics," *International Journal of Space Structures*, vol. 36, no. 2, pp. 105–116, 2021.

[20] X. X. Cheng and Z. Y. Song, "Modal experiment and model updating for Yingzhou Bridge," *Structures*, vol. 32, pp. 32746–32759, 2021.

[21] C. Natalicchio, H. Al-Khateeb, M. J. Chajes, Z. Y. Wu, and H. W. Shenton III, "Model calibration of a long-span concrete cable-stayed bridge based on structural health monitoring data: influence of concrete variability," *Bridge Structures*, vol. 18, no. 1-2, pp. 45–62, 2022.

[22] Z. Xia, A. Li, J. Li, H. Shi, M. Duan, and G. Zhou, "Model updating of an existing bridge with high-dimensional variables using modified particle swarm optimization and ambient excitation data," *Measurement*, vol. 159, Article ID 107754, 2020.

[23] D. Da-hua, H. Er-ming, and L. Lei, "A dynamics model updating method of nozzle based on improved simulation annealing algorithm," *Journal of Astronautics*, vol. 39, no. 06, pp. 632–638, 2018.

[24] L. Chao-qian and P. Jian-chao, "Application of new simulated annealing genetic algorithm in path optimization," *Modular Machine Tool & Automatic Manufacturing Technique*, vol. 12, no. 03, pp. 52–55, 2022.

[25] R. I. Levin and N. A. J. Lieven, "Dynamic finite element model updating using simulated annealing and genetic algorithms," *Mechanical Systems and Signal Processing*, vol. 12, no. 1, pp. 91–120, 1998.

[26] Z. Changlin, Y. Jianxing, and Y. Zhenguo, "Nonlinear constraint optimization problem of multi-objective simulated annealing algorithm," *Journal of Fudan University (Natural Science)*, vol. 42, no. 01, pp. 93–97, 2003.

[27] X. Yu, *Nonlinear Structural Model Updating Based on the Instantaneous Characteristics of Decomposed Dynamic Responses*, Hefei University of Technology, Hefei, China, 2016.

[28] P.-P. Yuan, W.-X. Ren, and J. Zhang, "Dynamic tests and model updating of nonlinear beam structures with bolted joints," *Mechanical Systems and Signal Processing*, vol. 126, pp. 126193–126210, 2019.

[29] Z. Wang, H. Yin, and Z. Peng, "Bayesian model updating based on kriging surrogate model and simulated annealing algorithm," *Journal of Physics: Conference Series*, vol. 2148, no. 1, Article ID 012008, 2022.

[30] H. Fang and M. F. Horstemeyer, "Global response approximation with radial basis functions," *Engineering Optimization*, vol. 38, no. 4, pp. 407–424, 2006.

[31] S. Yunkang and Y. Huiping, *Improvement of Response Surface Method and its Application to Engineering Optimization*, Science Press, Beijing, China, 2010.

[32] Ministry of Transport of China, *Code for Design of Reinforced concrete and Prestressed concrete Bridges and Culverts for Highway*, China Communications Press, Beijing, China, 2018.